NUMERICAL SIMULATION OF A SUPER-RADIANT THz SOURCE DRIVEN BY FEMTOSECOND ELECTRON BUNCHES*

R. Chulkov, B.I. Stepanov Institute of Physics, NAS, Minsk, Belarus
V. Goryashko, Department of Physics and Astronomy, Uppsala University, Uppsala, Sweden
V. Zhaunerchyk, Department of Physics, University of Gothenburg, Sweden

Abstract

We summarize our studies for a super-radiant source operating in the THz frequency range. In particular, we focus on a single-pass planar undulator comprising no guiding structure. Using a numerical code that supports 3D time-dependent modeling of radiated fields as well as statistical properties of electron bunches, we analyze influence of electron bunch parameters on generated THz radiation and reveal some surprising results. More specifically, for the considered undulator configuration, we predict degradation in the angular divergence and spectral broadening of the generated radiation as the electron bunch emittance decreases. We also demonstrate how electron bunch lengthening associated with the electron energy spread can be suppressed.

INTRODUCTION

Pulsed THz free-electron lasers (FELs) are typically driven by radio-frequency linear accelerators (rf Linacs) able to produce intense electron bunches with a duration in the picosecond or even in the femtosecond range. When the bunch length is much shorter than the resonant wavelength of an excited electromagnetic field in an undulator, the bunch radiates like a point-charge giving rise to the so-called super-radiant regime of an FEL [1]. In this case, output intensity scales as a squared number of all electrons at the FEL start-up while for SASE (self-amplified spontaneous emission) it scales with a number of electrons [2]. The super-radiant regime enables realization of a relatively compact high-power THz FEL facility based on a single-pass undulator configuration. At the same time, the operation efficiency of such a super-radiant source is strongly affected by the quality of a driving electron bunch such that the source design requires a numerical modeling, which should take into account general statistical properties of electron bunches as well as the THz field diffraction. Below, we present results of such a modeling for a single-pass THz super-radiant source comprising a planar undulator.

MODEL DESCRIPTION

Our numerical model describes a single-pass interaction geometry without any guiding structure for generated THz field. A numerical code accounts for a non-zero bunch emittance and an electron energy spread and enables 3D modeling of radiated fields when electron bunches are comparable to or shorter than the FEL resonant wavelength. The key approach of the model is the expansion of a THz field into complete sets of mutually orthogonal Hermite-Gaussian modes. The fast-varying field in a time domain is calculated via inverse Fourier transform of the frequency components. Details of our approach can be found in Refs. [3–8]. The model considers only a single linear polarization of the THz radiation lying in the plane of the wiggling motion of electrons. We also assume that the injected electron bunch is not astigmatic and its waist is located at the undulator center in the ballistic approximation. Then, the initial rms (root-mean-squared) bunch width $\sigma_{x,y}$ can be written as [9]:

$$\sigma_{x,y} = \sqrt{\epsilon\left(\beta_0 + \frac{L_u^2}{4\beta_0}\right)}, \tag{1}$$

where ϵ is the rms bunch emittance, β_0 is the geometrical β-function and L_u is the undulator length. An initial distribution of macroparticles in an electron bunch was simulated using a charge weighted algorithm based on the temporal Poisson statistical properties of electrons [10]. A Gaussian statistics is used to produce an initial energy spread and transverse distribution of the macroparticles. Their initial transverse velocities $[v_{0xj}, v_{0yj}]$ have been taken according to the relations [9, 11]:

$$v_{0xj} = -\vartheta x_{0j} v_{0zj}, \quad v_{0yj} = -\vartheta y_{0j} v_{0zj}, \tag{2}$$

$$\vartheta = \frac{1}{\beta_0}\left(\frac{L_u}{2\beta_0} + \frac{2\beta_0}{L_u}\right)^{-1}, \tag{3}$$

where $[x_{0j}, y_{0j}]$ are the initial transverse coordinates of the macroparticles. The numerical code has been implemented in the double precision arithmetic. The finite-difference integration scheme of the equations for electron motion as well as the equations for the Fourier amplitudes is the 4-th order Bashforth-Moulton predictor-corrector [12] with relative tolerance control on each integration step. Parameters of the simulations are listed in Table 1.

Table 1: Parameters of the Simulation

resonant frequency, THz	0.3	1.0	3.0
bunch charge, nC	1.0	1.0	0.5
mean e-energy, MeV	9.0	9.31	16.5
bunch duration, fs	150	150	100
bunch β_0-function, m	3.0	3.0	3.0
magnetic flux, T	0.31	0.14	0.14
undulator period, cm	11.0	11.0	11.0
number of periods	9	9	9
undulator parameter K_u	2.26	1.0	1.0

* Work supported by the Swedish FEL center

ISBN 978-3-95450-133-5

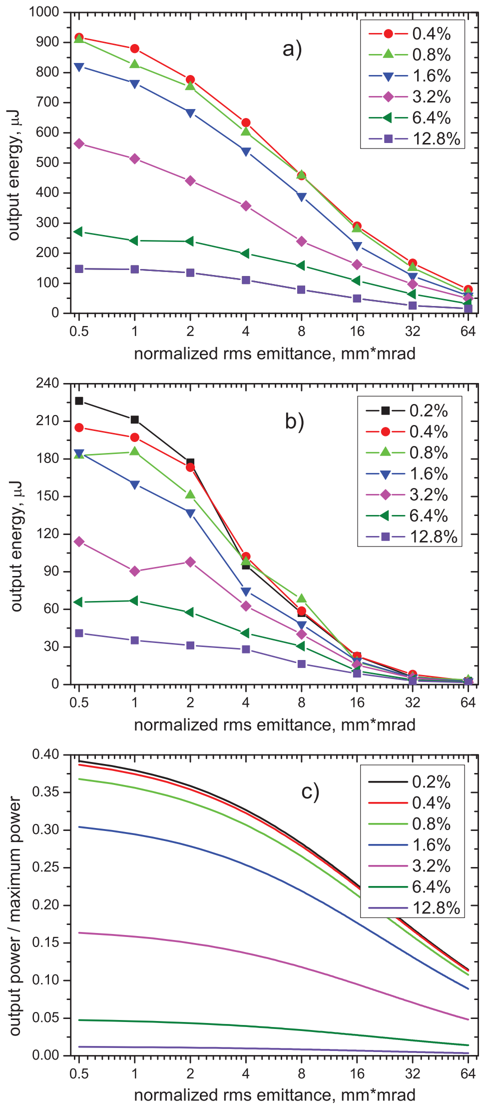

Figure 1: (Color online) The output energy of THz pulses as a function of ϵ_n for different δ-values at f_R=0.3 THz (a) and f_R=3.0 THz (b). The relative THz power is analytically evaluated for f_R=3.0 THz (c).

RESULTS

Figure 1a shows the output energy E_{THz} of THz pulses calculated as a function of the normalized bunch emittance ϵ_n for different values of the relative energy spread δ and resonant frequency f_R=0.3 THz. As one can see, the output energy E_{THz} is highly sensitive to both the bunch emittance and energy spread. For the high-quality electron bunch with ϵ_n <1 mm·mrad and δ <1%, the model predicts an output energy up to 1 mJ that corresponds to the conversion of the electron bunch energy into radiation of more than 10% . This value is approximately an order of the magnitude higher than typical conversion efficiencies of short-pulse THz FEL oscillators [7, 8]. We explain this by the fact that in a super-radiant source, electrons lose their energy coherently as long as the bunch length is far less than the resonant wavelength. Under these conditions, the electron energy loss results in shift of the resonant wavelength to lower frequencies according to the FEL resonant condition. This is the case of low emittance and energy spread. However, when the bunch quality degrades, the scatter in the longitudinal velocities of electrons leads to the bunch lengthening when electrons in different parts of the bunch oscillate with a different phase. The relative electron phase reaches π-value when the bunch length approaches a half of the resonant wavelength or exceeds it. Under such conditions, the mutual coherence between different part of the bunch gets broken and the output energy drops drastically (Fig. 1a). Thus, E_{THz}<100 μJ for ϵ_n>50 mm·mrad regardless of the δ values. For ϵ_n ≈5 mm·mrad, the same E_{THz} values are also predicted when δ>13%.

For resonant frequency f_R=1.0 THz, our model predicts nearly the same level of the peak output energy, E_{THz}>0.8 mJ. However, in this case, the energy is more sensitive to the bunch quality. This is because of a shorter resonant wavelength and more stringent requirements to a tolerable scatter in electron velocities. For f_R=3.0 THz, we did not observe any noticeable output for a bunch duration of 150 fs since, under such conditions, the bunch length was close to the FEL resonant half-wavelength. Figure 1b shows numerical results obtained for 100 fs bunch duration. In comparison with the data shown in Fig. 1a, there is a noticeable decrease in E_{THz}, that does not exceed 0.3 mJ even if the super-radiant source is driven by high-quality electron bunches. For moderate-quality bunches (δ = 4% and ϵ_n = 20 mm·mrad), predicted E_{THz} value is only ~8 μJ.

A comparison of the numerical data with the prediction of the analytical theory [14] (Fig. 1c) indicates that the numerical model is more sensitive to ϵ_n but it is less susceptible to δ. Specifically, the calculated output energy drops 8.2 times whereas the theoretical power does 2.3 times as ϵ_n increases from 0.5 to 32 mm·mrad. When δ increases from 0.2 to 6.4%, the calculated energy and the theoretical power gain drops 3.3 and 8.3 times, respectively. The discrepancy between the numerical and theoretical dependencies can be explained by the fact that at relatively low ϵ_n values, the electron bunch lengthening caused by a non-zero electron energy spread can be suppressed (Fig. 2). Such suppression is directly related to the bunching effect of the generated THz wave, which tends to group electrons in such a way that they are pulled into regions of the peaks of the electric field. This bunching enhances electromagnetic emission at low ϵ_n when the electron current density is relatively high. However, at high ϵ_n or low current density, the intensity of the THz field is insufficient for electron bunching, see Fig. 2(a).

Figure 3 shows the normalized THz spectra calculated at f_R=3.0 and 1.0 THz. The undulator parameter K_u is equal to 1.0 for all the cases presented and no evident high-order spectral harmonics are observed. As is seen, all the spectral distributions are extended from the resonant frequency towards the low-frequency side. The resonant frequency appears as a cut-off value above which spectral intensities di-

ISBN 978-3-95450-133-5

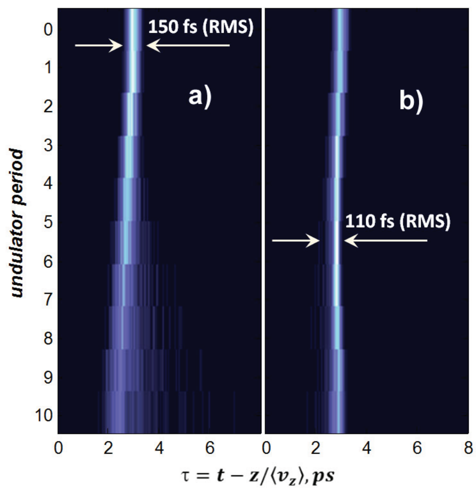

Figure 2: (Color online) The density maps of electron trajectories in a coasting frame calculated for ϵ_n=64 mm·mrad (a) and ϵ_n=4 mm·mrad (b) when δ=1% and f_R=1.0 THz.

minish to almost zero. Causes of such spectral extension to low-frequencies will be discussed below and here we just mention that an increase in duration of a driving electron bunch leads to additional broadening of the spectrum and frequency down shift of its peak intensity. For instance, at f_R=3.0 THz the relative width of a super-radiant pulse exceeds 100% when the bunch duration is greater than 100 fs (Fig. 3a). The spectral broadening with an increase in the bunch duration is due to enhanced contribution of SASE for which an effective interaction length with the electron bunch is less than the undulator length due to diffraction walk-off out of the interaction region. Similar broadening is also observed when δ grows. In this case, however, the shift of the peak spectral intensity is negligible (Fig. 3b).

The spectral changes due to the variation in ϵ_n require a more detail discussion. Figure 3c demonstrates that a decrease in ϵ_n leads to both the shift in the peak intensity and spectral broadening. However, the cause of such a broadening is quite different from the above two cases. It turned out that this spectral behavior is directly related to spatial properties of the generated radiation. In order to reveal its physical origin, we calculated the output transverse energy density distributions of the THz radiation for low and high ϵ_n values, which are shown in Fig. 4a and Fig. 4b, respectively. The former exhibits a broad halo of more than the 50 mm width. In the second case, the THz beam width is several times narrower (~10 mm, FWHM) and despite pronounced astigmatism in its transverse profile, it is close to a Gaussian distribution both in vertical and horizontal directions. The spatially broadened THz field at the undulator output at the low ϵ_n value is due to the enhanced off-axial field contribution. This contribution grows with an increase in the diffraction angle $\alpha_d = c/(2\pi f w_0)$, which is in inverse proportion to the transverse width w_0 of the region where electrons emit coherently.

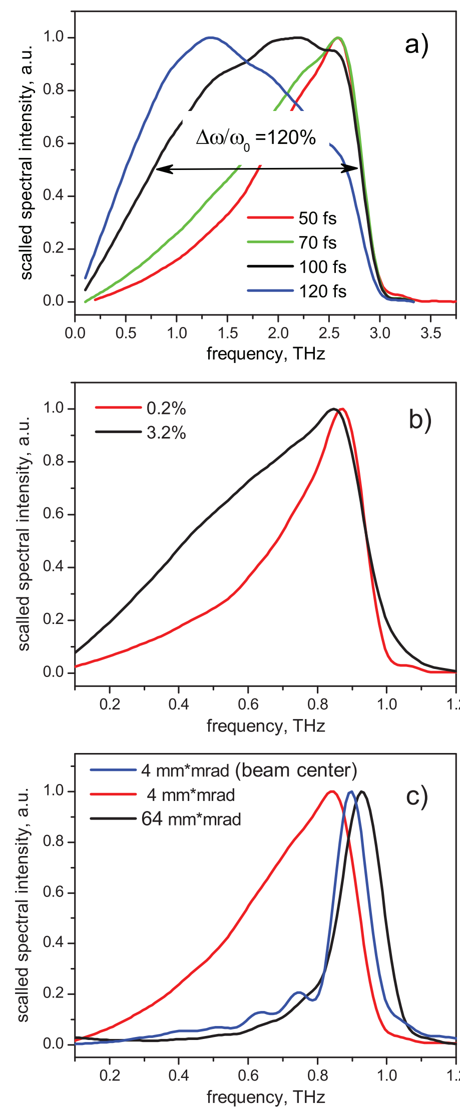

Figure 3: (Color online) The scaled output spectra calculated for different bunch durations at f_R=3.0 THz, δ=1%, and ϵ_n=4 mm·mrad (a); for two δ values at f_R=1.0 THz and ϵ_n=8 mm·mrad (b); for two ϵ_n values at f_R=1.0 THz and δ=1% (c).

The off-axial FEL resonant condition shifts f_R to the lower values with an increase in the angle between observation direction and the undulator axis [13]. Thus, when ϵ_n decreases, the w_0 value decreases as well (Eq. 1c) giving rise to the spatial divergence of the THz radiation that leads to enhanced off-axial intensity and spectral broadening. Such a conclusion is supported by comparison of the THz spectra calculated at ϵ_n=4 mm·mrad over the transverse region of 80 × 80 mm and a paraxial part, which is confined by 10 × 10 mm. The paraxial spectrum is considerably narrower and its peak intensity is close to the f_R value (Fig. 3c).

The spectra of the super-radiant THz radiation shown in Fig. 3 are given for the undulator parameter $K_u = 1$ such that no evident high-order harmonics are recognized.

ISBN 978-3-95450-133-5

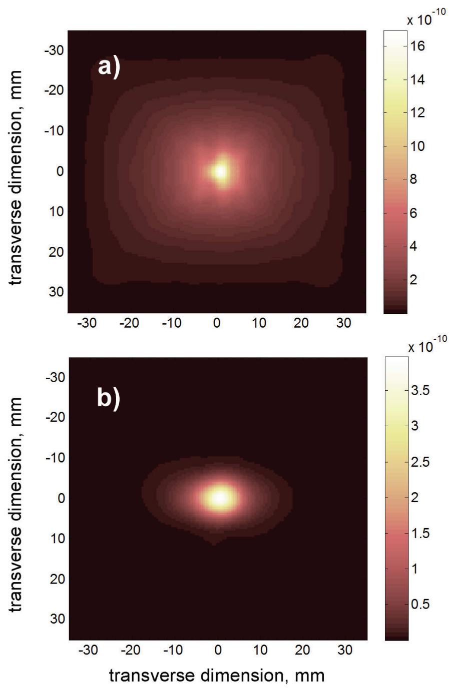

Figure 4: (Color online) The density map of a transverse distribution of radiated energy calculated for f_R=1.0 THz, δ=1%, ϵ_n=4 mm·mrad (a) and ϵ_n=64 mm·mrad (b).

Meanwhile Fig. 5 demonstrates the spectrum calculated for f_R=0.3 THz and $K_u \approx 2.3$. One can clearly see both odd and even frequency harmonics in the spectrum. Note that the paraxial spectrum is enriched by odd harmonics whereas even harmonics are more intensive in the integral spectrum. This observation agrees with the FEL theory for the off-axial light generation [13].

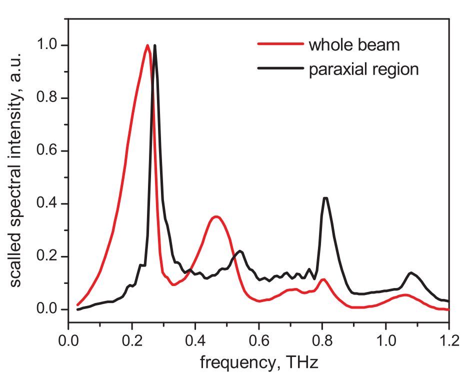

Figure 5: (Color online) The scaled output spectra of the whole super-radiant pulse and only of a paraxial region calculated for f_R=0.3 THz, δ=1%, ϵ_n=4 mm·mrad.

CONCLUSION

We have analyzed radiation properties of an single-pass super-radiant THz source having a simple undulator with plane magnets. The comparison of the analytical and numerical results indicates that our numerical model predicts the radiation output to be more sensitive to the bunch emittance but less susceptible to the electron energy spread. The discrepancy is related to the bunching effect of the THz field on electrons that enhances the FEL output at low emittance values. We have also investigated the impact of the electron bunch quality on spectral and spatial properties of the THz radiation and shown that the increase in the bunch duration and electron energy spread leads to the spectral broadening. The cause of such a spectral broadening is the enhanced contribution of SASE. For the considered interaction geometry, we predict degradation in angular divergence of the generated radiation and its spectral broadening as the electron bunch emittance decreases. Such degradation and broadening have been shown to be directly related to the diffraction and the FEL resonance condition for off-axis light generation.

ACKNOWLEDGMENT

We would like to acknowledge the financial support from the Swedish FEL center.

REFERENCES

[1] A. Gover, F. V. Hartemann, G. P. Le Sage, N. C. Luhmann, R. S. Zhang, and C. Pellegrini, Phys. Rev. Lett., **72**, 1192 (1994).

[2] R. Bonifacio and F. Gasagrande, Nucl. Instrum. Methods A, **239**, 29 (1985).

[3] Y. Pinhasi, V. Shterngartz, and A. Gover, Phys. Rev. E **54**, 6774 (1996).

[4] Y. Pinhasi, Yu. Lurie, and A. Yahalom, Nucl. Instrum. Methods Phys. Res., Sect. A **475**, 147 (2001).

[5] M. J. de Loos, C. A. J. van der Geer, S. B. van der Geer, A. F. G. van der Meer, D. Oepts, and R. Wünsch, Nucl. Instrum. Methods Phys. Res., Sect. A **507**, 97 (2003).

[6] V. Zhaunerchyk, R. T. Jongma, Yu. Lurie, Y. Pinhasi, and W. J. van der Zande, Appl. Phys. Lett. **97**, 231109 (2010).

[7] V. Zhaunerchyk *et al.*, Phys. Rev. Spec. Top. Accel. Beams **15**, 050701 (2012).

[8] R. Chulkov, V. Goryashko, D. Arslanov, R. T. Jongmac, W. J. van der Zandec, and V. Zhaunerchyk, Phys. Rev. Spec. Top. Accel. Beams, **17**, 050703 (2014).

[9] D. A. Edwards, M. J. Syphers, An Introduction to the Physics of High Energy Accelerators, Wiley (1993).

[10] B.W. J. McNeil, M.W. Poole, and G. R.M. Robb, Phys. Rev. Spec. Top. Accel. Beams, **6**, 070701 (2003).

[11] G. Mishra, V. Gupta, N. P. Rajput, B. Kuske, D. Kraemer, R. Bakker, Nucl. Instr. Meth. Phys. Res. A **527**, 233 (2004).

[12] W. H. Press et al., Numerical recipes in FORTRAN (second edition), Cambridge University Press (1992).

[13] G. Dattoli, A. Renieri, A. Torre, Lectures on the Free Electron Laser Theory and Related Topics, World Scientific, 637 pages (1993).

[14] R. Bonifacio, L. De Salvo Souza, B.W.J. McNeil, Opt. Commun. **93**, 179 (1992).

ISBN 978-3-95450-133-5